Vibration Characteristic Analysis and Optimization of Heavy Load High Voltage Circuit Breaker Contact

Aibin Zhu[1(✉)], Wencheng Luo[1], Jianwei Zhao[2], and Dayong He[1]

[1] Key Laboratory of Education Ministry for Modern Design & Rotor-Bearing System, Xi'an Jiaotong University, Xi'an 710049, China
abzhu@mail.xjtu.edu.cn,
{luo0409,hedayong}@stu.xjtu.edu.cn
[2] School of Mechanical Electronic and Information Engineering, China University of Mining and Technology (Beijing), Beijing 100083, China
zhaojianwei@cumtb.edu.cn

Abstract. The steady and rapid action of contact directly determines the overall performance of high voltage circuit breaker robot in closing and opening process. The current high-voltage circuit breaker robot reveals obvious contact vibration during use. In order to alleviate the ablation of contact due to the electric arc which is caused by the contact vibration, this essay establishes a forced vibration model of damped three degrees of freedom system through citing a new high-voltage circuit breaker, and analyzes the impacts of the mass and equivalent stiffness proportion among static contact, moving contact and support frame on the contact vibration frequency and amplitude by adopting Dunkerly and matrix iteration methods. Through adding vibration measuring instrument in the contact for experimental verification, the results show that appropriate and reasonable optimization of the mass proportion and equivalent stiffness proportion among static contact, moving contact and support frame can effectively reduce the amplitude of the first order of the main vibration mode, thus significantly alleviating the ablation of contact under the premise of effectively ensuring the opening speed to meet the conditions. The study results can remarkably reduce the vibration of high voltage circuit breaker contact, and then improve the overall performance of high voltage circuit breaker robot.

Keywords: High voltage circuit breaker · Three degrees of freedom system · Equivalent stiffness · The first order vibration mode · Opening speed

1 Introduction

High voltage circuit breaker (hereafter referred to as HVCB) is an important control and protection robot in the power system, its main role is to effectively control and protect power transmission lines and electrical apparatus [1–3]. In order to meet the

A. Zhu, W. Luo, J. Zhao and D. He — Co-first authors: they contribute equally to this research.

L. Zhang et al. (Eds.): AsiaSim 2016/SCS AutumnSim 2016, Part II, CCIS 644, pp. 11–19, 2016.
DOI: 10.1007/978-981-10-2666-9_2

kinetic characteristic of contact, the closing speed must be quick enough to decrease the arcing time of pre-breakdown, so as to alleviate the ablation of contact surface [4, 5]. But on the other hand, excessive closing speed will cause contact vibration which also can leads to the ablation of contact surface. Therefore, the vibration characteristics simulation of HVCB contact can help to ease the closing elastic vibration, opening bounce [6], and improve the working life of HVCB robot.

In terms of reducing the contact vibration of HVCB robot, the domestic scholars have done some preliminary studies. Yang-Wu carried on the theoretical analysis and simulation of hydraulic operating mechanism opening buffer [7]. Xu-Jian Yuan established the relationship among the speed characteristic, contact overshoot and rebound amplitude, and achieved effective inhibition of contact overshoot and bounce through calibrating the default value [8]. Qian-Jia Li analyzed the impact phenomena and calculation methods of moving component of HVCB operating mechanism during processing, and analyzed the best mass ratio of the two colliding part under the different requirements [9]. Lin concluded that increasing contact spring stiffness coefficient can limit the closing vibration [10]. Zhang et al. [11], Fu and Hao [12] researched the fault diagnosis methods based on vibration signal.

The above research results are effective for simple operation system, especially for low-voltage circuit breaker mechanism motion characteristics where opening speed is not seen as important. However, it is dramatically difficult to obtain good vibration damping effect for HVCB robot with intricate mechanical structure and numerous mechanical components. Besides that, this method will prolong design cycle and augment the product cost. Especially for heavy load HVCB robot researched in this paper, the structure is shown in Fig. 1, and the comparison parameter with the traditional CT20 HVCB is shown in Table 1. It can be seen from the Table 1 that the new type circuit breaker can endure 550 kV voltage level or higher voltage level, and the closing spring operating power is nearly 6KN, which is almost twice what the

Table 1. The parameter comparison between CT20 HVCB and new type HVCB

Parameter comparison	Opening power/KN	Closing power/KN	Opening speed/m/s	Closing speed/m/s	Applied voltage grade/KV
CT20	1.8	3.2	4.5 ~ 5.5	2.5 ~ 3.5	40 ~ 252
New type	3.8	5.9	7.8 ~ 9.2	3 ~ 4	550 ~ 800

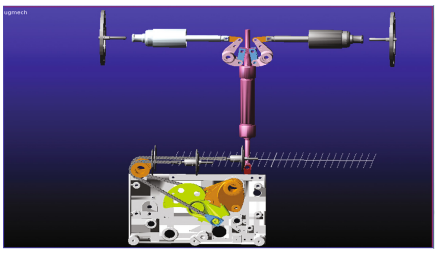

Fig. 1. The structure of high voltage circuit breaker

traditional CT20 HVCB can provide. Additionally, the new type HVCB has more than 300 components and fast closing speed, it needs to endure bigger closing impact with, so the method of adding buffer almost has no effect on the new circuit breaker.

Given that the contact vibration condition, this essay establishes a forced vibration model of damped three degrees of freedom system based on vibration mechanics theory, and analyzes the impacts of the mass and equivalent stiffness ratio among static contact, moving contact and support frame on the contact vibration frequency and amplitude by adopting Dunkerly and matrix iteration methods. Through adding vibration measuring instrument in the contact for experimental verification, the results show that reasonable optimization of the mass and equivalent stiffness ratio among static contact, moving contact and support frame can effectively reduce the amplitude of the first order vibration mode, thus significantly alleviating the ablation of contact.

1.1 The Establishment of Vibration Mechanical Model

Motion differential equation of damped multiple-degree-of-freedom system is Eq. (1):

$$M\ddot{x} + C\dot{x} + Kx = P(t) \tag{1}$$

Where mass matrix M, stiffness matrix K, damping matrix C are all $n \times n$ square matrices, x, $\dot{x}$, $\ddot{x}$ and $P(t)$ are all n-dimensional vector. The specific form of reaction equation as the following:

$$\begin{bmatrix} m_{11} & m_{12} & \cdots & m_{1n} \\ m_{21} & m_{22} & \cdots & m_{2n} \\ \vdots & \vdots & \ddots & \vdots \\ m_{n1} & m_{2n} & \cdots & m_{nn} \end{bmatrix} \begin{bmatrix} \ddot{x}_1 \\ \ddot{x}_2 \\ \vdots \\ \ddot{x}_n \end{bmatrix} + \begin{bmatrix} c_{11} & c_{12} & \cdots & c_{1n} \\ c_{21} & c_{22} & \cdots & c_{2n} \\ \vdots & \vdots & \ddots & \vdots \\ c_{n1} & c_{2n} & \cdots & c_{nn} \end{bmatrix} \begin{bmatrix} \dot{x}_1 \\ \dot{x}_2 \\ \vdots \\ \dot{x}_n \end{bmatrix} + \begin{bmatrix} k_{11} & k_{12} & \cdots & k_{1n} \\ k_{21} & k_{22} & \cdots & k_{2n} \\ \vdots & \vdots & \ddots & \vdots \\ k_{n1} & k_{2n} & \cdots & k_{nn} \end{bmatrix} \begin{bmatrix} x_1 \\ x_2 \\ \vdots \\ x_n \end{bmatrix} = \begin{bmatrix} P_1(t) \\ P_2(t) \\ \vdots \\ P_n(t) \end{bmatrix} \tag{2}$$

Where c_{ij} in the matrix C is called the damping influence coefficient, its meaning is the corresponding force applied on the i-coordinate to make the system generate unit speed only on the j-coordinate.

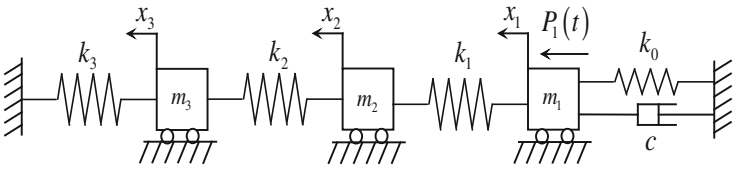

Fig. 2. Forced vibration model of damped three degrees of freedom system

In Fig. 2, the paper establishes a forced vibration model of damped three degrees of freedom system. In the process of collision, the moving contact m_1 under the force

$P_1(t)$ collides with the static contact m_2, the support frame of the static contact is m_3. Respectively, the equivalent spring stiffness between moving contact and static contact is k_1, between the stationary contacts and the support frame is k_2 and between the support frame and the ground is k_3.

Combined with the Eqs. (1) and (2) to obtain the specific form of the forced vibration model's motion equation, the matrix form of the differential equation as the following:

$$\begin{bmatrix} m_1 & 0 & 0 \\ 0 & m_2 & 0 \\ 0 & 0 & m_3 \end{bmatrix} \begin{bmatrix} \ddot{x}_1 \\ \ddot{x}_2 \\ \ddot{x}_3 \end{bmatrix} + \begin{bmatrix} c & 0 & 0 \\ 0 & 0 & 0 \\ 0 & 0 & 0 \end{bmatrix} \begin{bmatrix} \dot{x}_1 \\ \dot{x}_2 \\ \dot{x}_3 \end{bmatrix} + \begin{bmatrix} k_1 + k_2 & -k_2 & 0 \\ -k_2 & k_2 + k_3 & -k_3 \\ 0 & -k_3 & k_3 \end{bmatrix} \begin{bmatrix} x_1 \\ x_2 \\ x_3 \end{bmatrix} = \begin{bmatrix} P_1(t) \\ P_2(t) \\ P_3(t) \end{bmatrix} \tag{3}$$

To solve the first-order vibration mode's natural frequency by adopting Dunkerly and matrix iteration methods [13], the completed method is demonstrated as the following. First, record $n \times n$ square matrix A as the dynamic matrix of the system, which is defined as $A = FM = K^{-1}M$. In order to prevent elements of the iteration vector become too big or too small during the iterative process, the vector needs to be normalized after each iteration step, i.e., replaces the last element with 1. The concrete calculating steps of matrix iterative method as the following:

(1) Select the initial iteration vector X_1, replace the last element with 1;
(2) Iterate matrix X_1, and make new vector Y_1 normalization;
(3) Repeat Eq. (4) iteration equation

$$Y_r = AX_r, X_{r+1} = \frac{1}{(Y_r)_n} Y_r \tag{4}$$

If there is $X_{r+1} = X_r$ within the permissible error range, take X_{r+1} or X_r as the first-order vibration mode. Therefore, the first order natural frequency is shown as the following:

$$\lambda_1 = \frac{(Y_r)_n}{(X_r)_n} = \frac{(Y_r)_n}{1}, \omega_1 = \frac{1}{\sqrt{(Y_r)_n}} = \frac{1}{\sqrt{\lambda_1}} \tag{5}$$

2 The Analysis of Contact Vibration Mechanical Model

Based on the previous analysis, the vibration mechanics characteristics of the contact is determined primarily by the mass of static contact m_1, moving contact m_2 and support frame m_3 and equivalent stiffness ratio k_1, k_2, k_3 between them. However, how will this six parameters affect the vibration characteristics of the contact and the influence extent need to be further explored and analyzed.

Barkan has made some discussion on dynamical processing of contact closing bounce [14]. He proposed a three degrees of freedom energy transmission model for the analysis of contact collision. The main result obtained from the model is that when $k_2/k_1 = 1 = m_3/m_1$, the kinetic energy associated with the collision can be transmitted and retained to the support frame to the full extent during the collision. On the basis of Barkan's work, the author further analyzes the impacts of the mass ratio m_3/m_2 and equivalent stiffness ratio k_3/k_1 on the contact vibration frequency and amplitude.

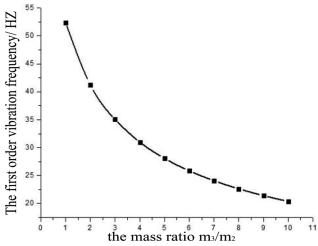

Fig. 3. The mass ratio influence

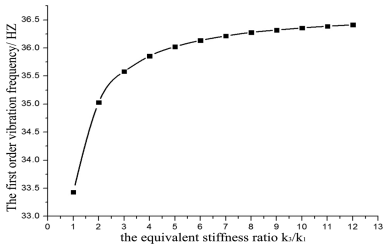

Fig. 4. The equivalent stiffness ratio influence

In order to quantitatively analyze the impact of the collision parts mass ratio on the first order of the vibration mode's natural frequency, this essay gradually increase the mass ratio m_3/m_2 from 1 to 10, and then calculate the natural frequency for each mass ratio. In Fig. 3, in the course of the mass ratio m_3/m_2 increasing step by step, the first order natural vibration frequency decreases first quickly, then slowly and finally levels off. The vibration frequency varies in a larger range from 52 Hz to 18 Hz. From the above analysis, it can come to the conclusion that through appropriately increasing the mass ratio between support frame and static contact, the vibration impact can be quickly transmitted to the support frame so as to weaken the contact vibration.

Similarly, in order to quantitatively analyze the impact of the equivalent stiffness ratio k_3/k_1 on the first order of the vibration mode's natural frequency, this essay gradually increase the equivalent stiffness ratio k_3/k_1 from 1 to 12, and then calculate the natural frequency for each equivalent stiffness ratio. In Fig. 4, in the course of the equivalent stiffness ratio k_3/k_1 increasing step by step, the first order vibration frequency increases first quickly, then slowly and finally levels off. The vibration frequency varies in a small range from 32 Hz to 37 Hz. From the above analysis, it can come to the conclusion that through appropriately decreasing the equivalent stiffness ratio, the vibration can be reduced. And the impact of the equivalent spring stiffness ratio on the main vibration frequency of the first order is less than the mass ratio on the vibration frequency.

Considering the double contact structure of the new type HVCB, it is measured by the physical prototype of HVCB: $m_2 = 22.174$ kg , $m_1 = 37.392$ kg , $m_3 = 67.764$ kg. Through increasing or decreasing the mass of non-critical structural components, the author readjusts the mass ratio among static contact, moving contact, flange plate and support frame. After optimization, $m_1 = 64.428$ kg , $m_2 = 21.276$ kg , $m_3 = 66.391$ kg. Taking the optimization of the flange plate mass as an example, the author reduces the

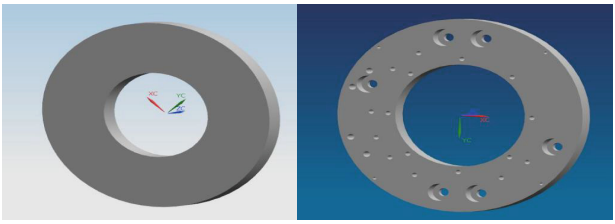

（a） Before optimizatio （b） After optimization

Fig. 5. The comparison of flange plate mass before and after optimization

flange plate overall mass through cutting holes in non-critical structural position as shown in Fig. 5. However, taking the real situation of mass ratio and material stiffness into account, the author finally determines $m_3/m_2 = 3$ and $k_3/k_1 = 10$ as the best approach.

3 The Results and Analysis of Contact Vibration Model Test

3.1 The Settings of Test Apparatus

In order to verify the accuracy of three degrees of freedom vibration model, the author conducts experiment research on the physical prototype of HVCB robot by using vibration analyzer. Through installing vibration sensors on the HVCB contact, the author respectively measures the contact vibration situation before and after the mass and equivalent stiffness optimization of static contact, moving contact, flange plate and support frame. And the author simultaneously records X direction transverse vibration of the contact in the process of opening and closing. Physical prototype and measurement method is shown in Fig. 6. Measuring principle is shown in Fig. 7.

Fig. 6. Measurement methods

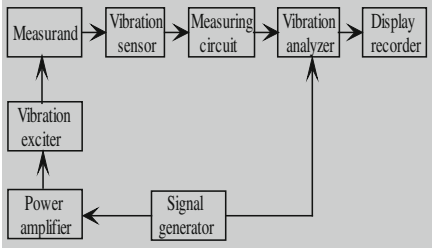

Fig. 7. Measuring principle

The author first sets 10 as the gradient for the range of 0 Hz to 100 Hz and 100 for the range of 100 Hz to 1000 Hz. Then under the different excitation vibration frequency, the author records the first order vibration frequency of contact and compares the experiment result with the model simulation result.

3.2 The Analysis of Experimental Results Before and After Optimization

The vibration response which is motivated by the external vibration in X direction is shown in Fig. 8. Before optimization, in the process of the excitation frequency gradually increasing from 0.1 Hz to 10 Hz, the amplitude increases slowly, then from 10 Hz to 30 Hz process, the amplitude increases rapidly, and there is a very remarkable peak at 31 Hz, from 31 Hz to 100 Hz, the amplitude decreases rapidly, and from 100 Hz to 1000 Hz, the amplitude slowly decreases to its original level. After the optimization, in the process of the excitation frequency gradually increasing from 0.1 Hz to 10 Hz, the amplitude increases slowly, then from 10 Hz to 20 Hz, the amplitude increases rapidly, and there is a very remarkable peak at 23 Hz, from 23 Hz to 100 Hz, the amplitude decreases rapidly, and from 100 Hz to 1000 Hz, the amplitude slowly decreases to its original level. Through the above analysis, it comes to the conclusion that the contact first order resonance frequency decreases from 31 Hz to 23 Hz after the optimization. The analysis shows the experimental results is consistent with the theoretic simulation results, and the maximum relative error is less than 5 %.

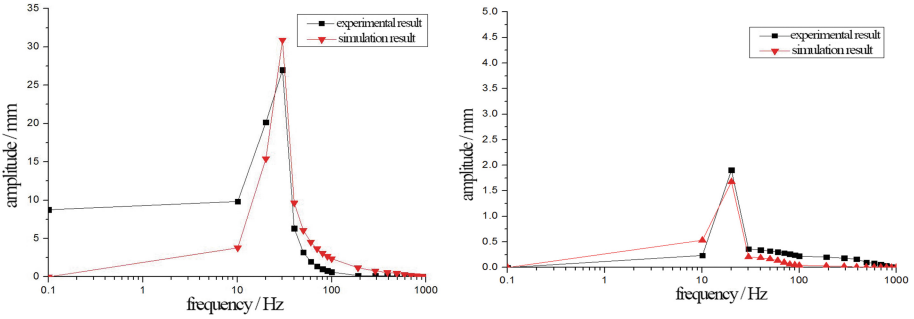

（a） Before optimization （b）After optimization

Fig. 8. The comparison of simulation and experiment results before and after optimization

Table 2. The comparison of simulation and experiment results before optimization

Performance parameter	Simulation	Experiment	Absolute error	Relative error/%
Frequency/Hz	22.74	23.61	0.87	3.67
Amplitude/mm	1.67	1.81	0.14	8.38

Table 3. The comparison of simulation and experiment results after optimization

Performance parameter	Simulation	Experiment	Absolute error	Relative error/%
Frequency/Hz	31.65	33.18	1.53	4.83
Amplitude/mm	30.89	28.46	2.43	7.87

As shown in Table 2, before optimization, the resonance amplitude measured by experiment is 28.46 mm and by simulation is 30.89 mm. Therefore, the simulation results agree with the experimental results essentially, and the maximum relative error of the average amplitude is less than 10 %. In Table 3, after optimization, the resonance amplitude measured by experiment is 1.81 mm and by simulation is 1.67 mm, and the maximum relative error of the average amplitude is less than 10 %. In conclusion, given that the experimental result curves agree with the simulation result curves better before and after optimization, the experiment results can prove the effectiveness of the forced vibration model simulation of damped three degrees of freedom system. In addition, after optimization, the ablation of the contact surface is greatly reduced and finally the service life of HVCB robot is improved.

Compared with the conclusion in Qian-Jia Li's essay [9], the kinetic energy associated with the collision can be transmitted and retained to the support frame to the full extent during the collision. Additionally, the mechanical transmission efficiency has been improved by 5 %.

4 Conclusion and Future Works

A forced vibration model of damped three degrees of freedom is proposed to achieve the contact vibration frequency and amplitude. Dunkerly and matrix iteration methods is adopted to calculate the first order vibration frequency. Both the simulation results and calculation results are verified by experiment. Experiment results show that the resonance amplitude of the physical prototype can be reduced from 28.46 mm to 1.67 mm after the optimization of the mass and equivalent stiffness proportion among static contact, moving contact and support frame, and the maximum relative error of average amplitude is less than 10 %. In conclusion, the study results can effectively reduce the amplitude of the first order of the main vibration mode, thus significantly alleviating the ablation of contact, and finally improve the overall performance of HVCB robot.

The future works of this study will continue the theoretical research on contact vibration model to further promote the performance of the heavy load HVCB. Meanwhile, the future works will concentrate on the ablation time to strengthen the approach of alleviating the ablation of contact.

References

1. Dai, Y., Zhang, M., Fan, K., et al.: Investigation of series-connected IGBTs in fast high-voltage circuit breaker. J. Fus. Energy **34**(6), 1406–1410 (2015)
2. Garzon, R.D.: High voltage circuit breakers: design and applications. Vacuum 214–218 (2002)
3. Zheng, X.-G.: Principle and application of high voltage circuit breaker, pp. 15–34. Tsinghua University Press, Beijing (2000)
4. Arabi, S., Trepanier, J.Y., Camarero, R.: Transient simulation of nozzle geometry change during ablation in high-voltage circuit breakers. J. Phys. D Appl. Phys. **48**(4), 22–114 (2015)

5. Godin, D., Trepanier, J.Y., Reggio, M., et al.: Modeling and simulation of nozzle ablation in high-voltage circuit-breakers. J. Phys. D Appl. Phys. **33**(20), 2583–2590 (2000)
6. Xu, K.X.: Optimization and simulation for spring actuator of high-voltage circuit breaker. Dalian Univ. Technol. 21–25 (2012)
7. Wu, Y., Zhe, R.-M., Chen, D.-G., et al.: Optimum design of high-voltage circuit breakers based on mechanism dynamic features simulation. J. Xi'an Jiaotong Univ. **36**(12), 1211–1214 (2002)
8. Yuan, X.-J., Lei-Wei, T.-G., et al.: Research on opening contact overshoot and rebound suppression methods of vacuum circuit breakers with permanent magnet actuator. High Volt. Appar. **51**(3), 22–27 (2015)
9. Li, Q.-J., Gang, G.-Y.: Analysis of mechanical impact in operating device for HV circuit breaker. High Volt. Appar. **39**(6), 20 (2001)
10. Lin, X., Cao, C., Bin, L.I., et al.: Dynamic simulation and opening bouncing analysis of vacuum circuit breaker with permanent magnetic actuator. High Volt. Appar. **39**(7), 1–5 (2013)
11. Zhang, P., Zhao, S.T., Shen, L., et al.: Research on vibration and acoustic joint mechanical fault diagnosis method of high voltage circuit breaker based on improved EEMD. Power Syst. Prot. Control **42**(8), 77–81 (2014)
12. Fu, C., Hao, J.: On-line monitoring system based on vibration signal of high voltage circuit breaker. J. Multimedia **9**(4), 598–603 (2014)
13. Ni, Z.-H.: Vibration Mechanics, pp. 277–286. Xi'an Jiaotong University Press, Xi'an (1989)
14. Barkan, P., Mcgarrity, R.V.: A spring-actuated, cam-follower system: design theory and experimental results. J. Manuf. Sci. Eng. **87**(3), 279–286 (1965)